Marine mixotrophy increases trophic transfer efficiency, mean organism size, and vertical carbon flux

Ben A. Ward[a,b,1] and Michael J. Follows[c]

[a]School of Geographical Sciences, University of Bristol, Bristol BS8 1SS, United Kingdom; [b]Laboratoire des Sciences de l'Environnement Marin, Institut Universitaire Européen de la Mer, Technopole Brest Iroise, 29280 Plouzané, France; and [c]Department of Earth, Atmospheric and Planetary Sciences, Massachusetts Institute of Technology, Cambridge, MA 02139

Mixotrophic plankton, which combine the uptake of inorganic resources and the ingestion of living prey, are ubiquitous in marine ecosystems, but their integrated biogeochemical impacts remain unclear. We address this issue by removing the strict distinction between phytoplankton and zooplankton from a global model of the marine plankton food web. This simplification allows the emergence of a realistic trophic network with increased fidelity to empirical estimates of plankton community structure and elemental stoichiometry, relative to a system in which autotrophy and heterotrophy are mutually exclusive. Mixotrophy enhances the transfer of biomass to larger sizes classes further up the food chain, leading to an approximately threefold increase in global mean organism size and an ~35% increase in sinking carbon flux.

mixotrophy | plankton | size | trophic transfer | biological pump

Marine ecosystems provide essential nutrition to more than half the world's population via fisheries (1) and mediate global cycles of climatically important elements including carbon (2). Current models of marine biogeochemical cycles assume that the plankton can be clearly divided into two mutually exclusive guilds: the autotrophic phytoplankton and the heterotrophic zooplankton. According to this view, phytoplankton are responsible for all photosynthetic carbon fixation, ultimately controlled by the supply and consumption of inorganic nutrients.

There is clear evidence that such a strict dichotomy between producers and consumers does not reflect the true nature of marine microbial communities. Autotrophic and heterotrophic traits are not mutually exclusive, and a large and increasing number of plankton taxa have been shown to simultaneously exploit both inorganic resources and living prey (3). These mixotrophic plankton, found throughout the eukaryotic tree of life (4), and particularly in the 2- to 200-μm size range (5–7), can sustain photosynthesis even when chronically outcompeted for the most-limiting inorganic nutrient, in clear contrast to the way we typically describe and model marine systems (8).

Although mixotrophy is known to be common throughout the global ocean (6, 7), its contribution to net community production is difficult to quantify, and its integrated impact on global biogeochemical cycles remains unknown. Numerical simulations provide a platform to address these questions, but to date, no global ocean models have resolved this important lifestyle. Here, we examine the global role of mixotrophy in a numerical "thought experiment," comparing two simulations of the marine plankton food web in the global ocean (9) that differ only in their representation of trophic strategy (Fig. 1). The traditional "two-guild" model encapsulates the default view of the marine ecosystem, with each of the 10 simulated size classes divided into separate phytoplankton and zooplankton populations. In the alternative "mixotrophy" model, this unrealistically strict distinction is not made, and each size class contains just one population that is capable of both inorganic resource uptake and predation, dependent on resource availability. A detailed model description can be found in the Supporting Information, Tables S1 and S2, and ref. 9.

Despite the removal of a distinction that is central to all current global-scale ecosystem and biogeochemistry simulations (9–12), the emergent community structure shown in Fig. 1B allows the mixotrophy model to reliably reproduce observed, global distributions of chlorophyll a, primary production and nutrients (Figs. S1 and S2). At specific time-series sites where in situ empirical data are available (Fig. S3), the two simulations show only minor differences in terms of their fidelity to observed seasonal cycles of chlorophyll a and limiting nutrients, whereas the mixotrophic model is better able to reproduce the concentrations of nonlimiting nutrients, which are often overestimated by the two-guild model.

Although the two model configurations make no prior assumptions with regard to the balance of autotrophic and heterotrophic nutrition in each size class, both model communities show a clear and credible (7, 9, 13) trophic structure, with a general shift from autotrophy to heterotrophy with increasing organism size and trophic level (Fig. 1 A and B). In each case, the smallest plankton are too small to ingest prey, whereas the largest plankton have very low affinities for inorganic nutrients. Alongside these similarities, there are also important differences, the most obvious being the strong disconnect between the first and second trophic levels seen in the two-guild model. With a strict dichotomy between phytoplankton and zooplankton, photosynthesis is restricted to the base of the food web, as shown in Fig. 1C. The flux of energy and biomass up the food chain decreases at each trophic level because the energetic demands of consumers can only be met by the catabolic respiration of ingested biomass. In the mixotrophic model, consumers can dramatically increase their apparent trophic transfer efficiency by using photosynthesis to compensate for respiratory losses. [An alternative mechanism not included in the model is the harvesting of light energy to decrease the need for catabolic respiration (14).]

Either mechanism allows greater transfer of energy and biomass across each trophic level, which ultimately supports greater

Significance

Marine plankton commonly combine the autotrophic use of light and inorganic resources with the heterotrophic ingestion of prey. These mixotrophs blur the strict boundary between producers and consumers and allow energy and biomass to enter the food web across multiple trophic levels. Incorporating this flexibility into a global simulation of the surface ocean food web reveals that mixotrophy enhances the transfer of biomass to larger organisms at higher trophic levels, which in turn increases the efficiency of oceanic carbon storage through the production of larger, faster-sinking, and carbon-enriched organic detritus.
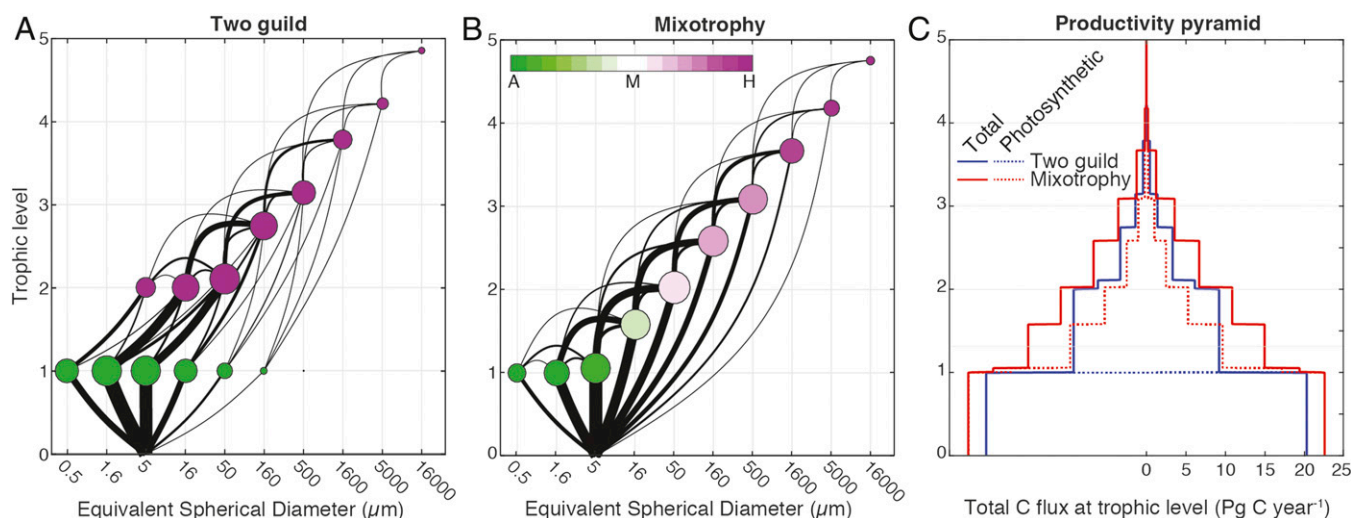
Fig. 1. Emergent global mean community structure in the two-guild (*A*) and mixotrophy (*B*) models. Circular nodes represent global carbon biomass (surface area proportional to the annual mean), and black links represent global carbon fluxes (thickness proportional to the square root of the annual mean, with all fluxes directed upwards). The horizontal position of the nodes denotes plankton size, whereas the vertical position denotes trophic level (*T*). For each population, *T* is calculated as 1 plus the average trophic level of each prey item, weighted by the contribution of each prey to the total carbon intake, including photosynthesis (*T* is calculated sequentially from small to large; *Methods*). Colors represent the balance of autotrophic and heterotrophic carbon assimilation in each population (*Inset*, color scale). (*C*) Representation of the total annual carbon flux across each trophic level in the two-guild (blue) and mixotrophy (red) models. The fluxes were calculated for each value of *T* by summing all fluxes beginning at a lower level and ending at a higher level. Solid lines represent the total flux, whereas dotted lines represent only the photosynthetic flux.

biomass among larger size classes further up the food chain (15). Fig. 2*A* shows that the total global biomass distribution is shifted toward larger size classes in the mixotrophy model, with an approximately threefold increase in global geometric mean plankton diameter (from 17 to 46 μm). Noting that both models neglect a range of other mechanisms that may also support photosynthetic growth among larger plankton (16), the inclusion of mixotrophy allows the model community to support much higher global values of primary production and chlorophyll *a* biomass in the 20- to 200-μm microplankton size range (Fig. 2*B*). This shift in community structure brings the mixotrophic model into closer agreement with empirical estimates derived from a synthesis of in situ and satellite observations (17, 18).

The shift toward larger plankton is ultimately driven by an increased competitive ability of mixotrophs relative to phytoplankton or zooplankton specialists. In general, the nutrient affinity of plankton decreases with increasing organism size (19), and in the two-guild paradigm, highly efficient uptake by the smallest

phytoplankton leaves insufficient nutrients to support photosynthesis in the larger groups. In the mixotrophy model, photosynthesis is supported among larger size classes because mixotrophs can exploit both inorganic nutrient resources and prey. Specifically, analytic solutions to a highly simplified version of the ecological model (*Methods*) show that the ability of mixotrophs to ingest prey not only provides an additional source of the nutrients required to support photosynthesis, but also provides an additional source of carbon as a supplement to photosynthesis. This double benefit decreases their dependence on inorganic nutrients and allows mixotrophs to survive at nutrient concentrations that would be unable to support specialist phytoplankton of equivalent size (*Methods* and Eq. **4**). The fact that this advantage is derived by eating smaller competitors (20) has the complementary effect of decreasing the biomass of smaller groups (Fig. 2*A*), further shifting the community mean toward larger sizes.

The flexible use of both inorganic and prey resources by mixotrophs is highlighted in Fig. 3, which shows the balance of
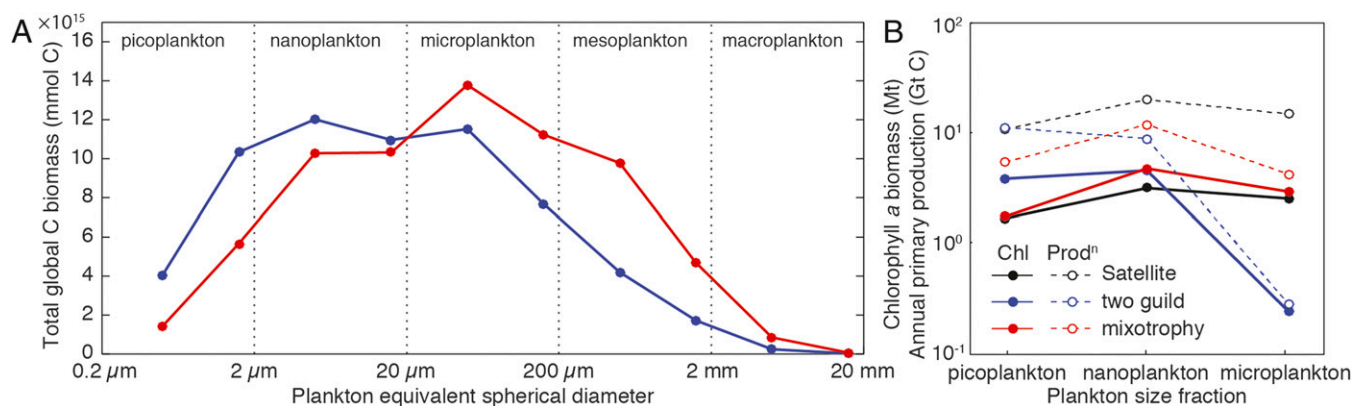
Fig. 2. (*A*) Total annual mean size distribution of carbon biomass in the two-guild (blue) and mixotrophy (red) models. (*B*) Global size-fractionated annual mean chlorophyll *a* biomass and annual primary production from the two-guild (blue) and mixotrophy (red) models in comparison with empirical estimates (black). Empirical estimates were derived from a synthesis of in situ and satellite observations (17, 18).

autotrophy and heterotrophy in the nanoplankton size class (selected because this intermediate size class is relatively evenly balanced between the two trophic strategies; Fig. 1 *A* and *B*). In the two-guild model, Fig. 3*E* shows that nanoplankton biomass is dominated at low latitudes by zooplankton. In these more stratified regions, and particularly at the centers of the subtropical gyres, the scarcity of any one nutrient resource allows the smaller picophytoplankton to outcompete the larger nanophytoplankton, in accordance with Liebig's law. The exclusion of nanophytoplankton leaves heterotrophy as the only viable strategy in the nanoplankton class, and all resources, including carbon, are acquired primarily by ingestion of prey (Fig. 3 *A–D*).

In the mixotrophic model, the nanoplankton mixotrophs are still outcompeted for limiting nutrients by the picoplankton at low latitudes, but the essential resource elements can be acquired instead by ingestion of prey (20). This flexibility is confirmed in Fig. 3 *G–I*, which shows that in regions where a nutrient is strongly limiting, the nanoplankton mixotroph community acquires that resource by grazing, for example, in the subtropical gyres for nitrogen and phosphorus, or in the equatorial Pacific for iron [black dots in Fig. 4 *G–I* show regions where each nutrient has been observed to be limiting, and model nutrient limitation is shown in Fig. S4]. This emergent feature of the simulations is consistent with experimental findings in the field and laboratory (5, 6, 21, 22). For example, equatorial Pacific isolates of *Ochromonas* species acquire iron by phagotrophy under iron-limited conditions (21), whereas photosynthetic protists acquire limiting N and P by phagotrophy in the North Atlantic (5, 6).
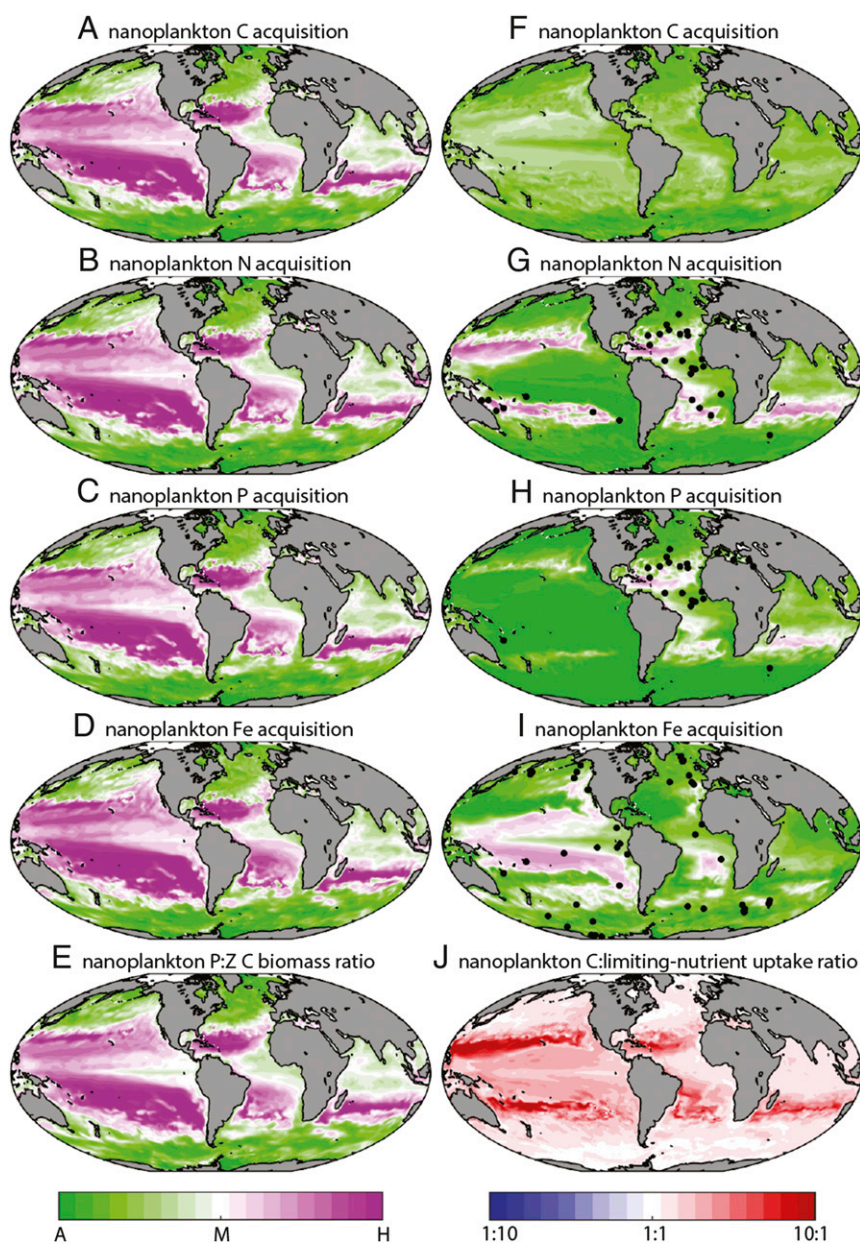

Fig. 3. (*A–D* and *F–I*) Depth-integrated balance of autotrophic and heterotrophic acquisition of C, N, P, and Fe by nanoplankton in the two-guild (*A–D*) and mixotrophy (*F–I*) models. Black dots in *G–I* indicate sites where in situ nutrient addition experiments have identified (at least occasional) limitation by that nutrient element (30). (*E*) Global balance of depth-integrated nanophytoplankton and nanozooplankton C biomass in the two-guild model. (*J*) Relative change between the two models in the molar ratio of photosynthetic C acquisition to the uptake of the most-limiting nutrient (N, P, or Fe; *Supporting Information*).
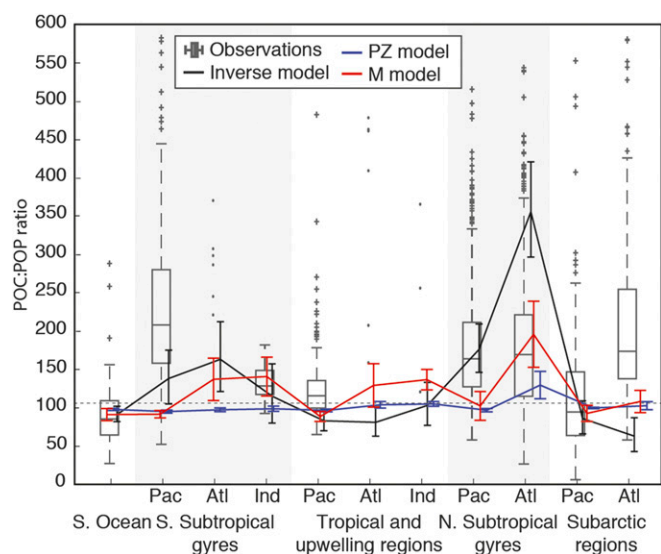
Fig. 4. Modeled and observed large-scale variation in C:P ratios of particulate organic matter. Blue and red lines show regional C:P in the surface 100 m, with error bars showing ±1 SD. Observed particulate C:P ratios from ref. 23 are shown, with boxes marking the 25th, 50th, and 75th percentiles and whiskers covering ~99.3% of the data. The remaining points are represented by plus symbols. Observations in regions with <10 data points are plotted individually (dots). Inverse model estimates of exported C:P ratios are also shown by black lines (24), with error bars again showing ±1 SD. The global mean "Redfield" (31) C:P ratio of 106 is shown by a horizontal dashed line.

The key difference in the mixotrophy model is that ingested nutrients are available to directly support photosynthesis in the nanoplankton (and larger) size classes in regions where light is abundant but nutrients are scarce. In contrast to the two-guild simulation, for which the nanoplankton are dominated by heterotrophs that must respire carbon for energy, the switch to mixotrophy allows this size class to support photosynthetic plankton that can accumulate much higher ratios of carbon to limiting nutrient elements. This broad shift in the trophic status of the larger plankton underpins the increased carbon content of particulates in the mixotrophic world.

Fig. 3F confirms that carbon acquisition by the mixotrophic nanoplankton is dominated by phototrophy throughout the surface ocean, regardless of whether the supply of inorganic N, P, or Fe is limiting to growth. This result is in clear contrast to the two-guild model, for which a shortage of any one of these inorganic nutrients is sufficient to suppress photosynthesis (Fig. 3A). The supplemental resources derived from prey allow the mixotrophic nanoplankton community to sustain higher levels of photosynthesis for a given supply of limiting inorganic nutrient, relative to the two-guild model. This can be seen quite clearly in Fig. 3J, which shows that mixotrophy universally increases the ratio of photosynthetic carbon fixation to the uptake of limiting inorganic nutrients. In a balanced system, this extra source of exogenous carbon leads to elevated carbon stoichiometry (Eq. 5), and Fig. 4 confirms that this mechanism allows the mixotrophy model to better reproduce the elevated C:P ratios seen in both suspended particulate (23) and exported (24) organic matter in the oligotrophic subtropical gyres.

The ability to supplement scarce nutrients through grazing allows mixotrophs greater flexibility to balance supply and demand (25) and leads to increased accumulation of carbon (and nonlimiting nutrients) relative to limiting nutrients. Coupled with the shift toward larger plankton size classes, which drives increased production of larger and faster sinking organic detritus, the increased relative carbon content of sinking organic material leads to an ~35% increase in global carbon export, relative to the two-guild model (from 7.2 to 9.8 Gt C yr^{-1}). It is likely, however, that this enhancement represents an upper limit, because in this initial simulation, mixotrophy was incorporated without consideration of any potential costs, and it seems intuitively unlikely that a mixotroph generalist could simultaneously achieve the same essential rates as similar phytoplankton and zooplankton specialists (26, 27).

The likely impacts of these potential tradeoffs were examined with additional simulations in which mixotrophs were placed in direct competition with phytoplankton and zooplankton specialists (i.e., with three competing populations within each size class). Across a number of model experiments (*Supporting Information* and Table S3), mixotrophy was associated with a range of costs, in the form of decreased resource acquisition rates relative to specialists. Fig. 5 confirms that increasing the assumed costs decreases both the relative importance of mixotrophy and the
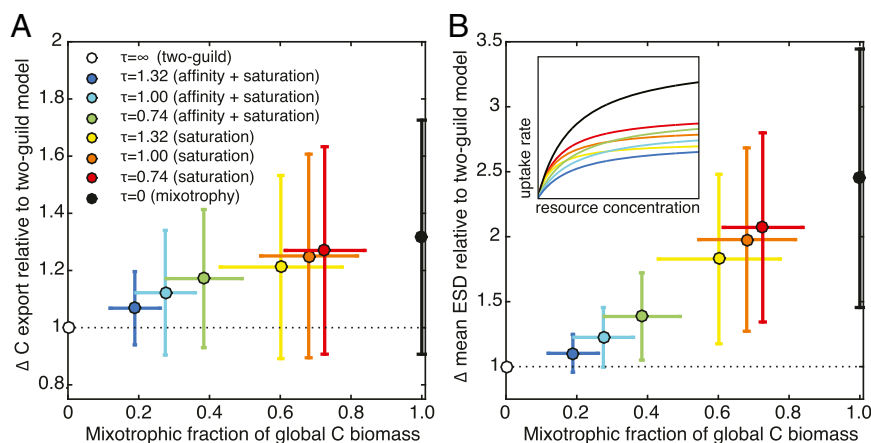
Fig. 5. Relationship between mixotrophic dominance and the relative increase in global carbon export (A) and global geometric mean plankton size (B) in the sensitivity experiments (*Supporting Information*), relative to the two-guild model. Dots represent the global average from each simulation, whereas the error bars show the degree of spatial variability in the annual average for each simulation. In the legend, the parameter τ describes the strength of the tradeoff (a larger number represents a stronger penalty for mixotrophy). This penalty may be applied to the resource affinities and the maximum resource uptake rates (affinity and saturation) or just to the maximum resource uptake rates (saturation) (*Supporting Information* and ref. 32). The relative uptake functions for the mixotrophs in each experiment are illustrated schematically in *B* (*Inset*). With no tradeoff, the mixotrophs have identical uptake functions to the specialists (black line).

inferred ecological and biogeochemical effects (Table S4). Nonetheless, Fig. 5 indicates that regardless of the tradeoffs, there is a clear positive relationship between the prevalence of mixotrophs and their impact on mean plankton size and carbon export. Given that mixotrophs are observed to be a ubiquitous component of marine food webs, Fig. 5 suggests that this prevalence should translate to significant ecological and biogeochemical impacts.

Although these numerical experiments suggest the potential importance of mixotrophy at the global scale, our representation of the mixotroph community is highly simplified, and many uncertainties remain. In particular, we have not differentiated among the wide diversity of different lifestyles and ecological strategies (such as the acquisition and use of ingested chloroplasts) that fall under the very broad classification of mixotrophy (4). In addition, computational constraints limited our global simulations to decadal timescales, and we did not address any longer-term feedbacks associated with the modified export of organic material. Alongside the increased export ratio of carbon to limiting nutrients, the simulations reveal increased export of nonlimiting nutrients, with elevated downward fluxes of organic N and P in regions where these elements are not limiting to growth. Over centennial and millennial timescales, this increased export may feedback on the supply of resources to the surface ocean, potentially modulating any short-term changes in C export. Further work in a simpler, less computationally expensive framework will be required to assess the potential for such indirect feedbacks.

Here we have presented a first effort to resolve mixotrophy in a global model of ocean ecology and biogeochemistry. The simulations are highly idealized and dependent on a number of uncertain physiological and ecological assumptions. Nonetheless, the results indicate a significant role for mixotrophy in shaping not only the structure of marine ecosystems but also the ecosystems' global-scale biogeochemical function. We suggest that existing carbon cycle models do not faithfully capture key mechanisms that shape trophic dynamics, elemental stoichiometry, and carbon export. An integrated approach combining targeted empirical studies with the explicit incorporation of mixotrophs into marine biogeochemical and global change models will therefore improve our quantitative understanding of marine food webs and the global carbon cycle.

Methods

Trophic Level. We use a standard definition of trophic level (28, 29), defined in terms of carbon and modified slightly to allow for mixotrophic nutrition. For a community of N plankton populations, the trophic level T_i of population i is given by

$$T_i = 1 + \sum_{j=1}^{N} T_j p_{ij}. \tag{1}$$

Here, T_j is the trophic level of each prey population j, and p_{ij} is the relative contribution of prey population j to the total carbon assimilation by population i (including photosynthesis). Whereas strict autotrophs have a trophic level of exactly 1, the trophic levels of mixotrophic or heterotrophic plankton are computed sequentially from the smallest to the largest groups. According to this definition, a strict herbivore consuming only strict autotrophs is assigned $T = 2$. Drawing nutrition from sources across multiple trophic levels allows populations to occupy intermediate trophic levels. For example, a mixotroph gaining exactly half of its organic carbon from photosynthesis and half through grazing on a strict autotroph ($T = 1$) would be assigned $T = 1.5$.

Simplified Analytic Model. The emergent behavior of the global model can be interpreted under a number of simplifying assumptions. Eq. S2 (*Supporting Information*) describes the rate of change of biomass for each plankton class, and we focus here in particular on carbon and phosphorus biomass (B_C and B_P). For simplicity, we look at the behavior of just one plankton size class in a homogenous physical environment, and we neglect mortality from higher predators to consider the balance between resource acquisition and basal mortality (m). Photosynthetic carbon fixation and predatory carbon assimilation are both down-regulated when the cellular quota becomes carbon enriched (phosphorus starved), whereas phosphate uptake and predatory phosphorus assimilation are up-regulated. Here, for simplicity, we assume that both the autotrophic and heterotrophic regulation terms are identical in each case.

$$\frac{dB_P}{dt} = \left(V_P^{max} \frac{P}{P + k_P} + G_C^{max} \frac{F_C}{F_C + k_g} \lambda Q_F \right) \left(\frac{Q_{max} - Q}{Q_{max} - Q_{min}} \right) B_C - m B_P, \tag{2}$$

$$\frac{dB_C}{dt} = \left(V_C + G_C^{max} \frac{F_C}{F_C + k_g} \right) \left(1 - \frac{Q_{min}}{Q} \right) B_C - m B_C. \tag{3}$$

Here, V_C represents the light-limited rate of photosynthesis, whereas Q represents the cellular P:C ratio, bounded by minimum and maximum values Q_{min} and Q_{max}. Phosphorus uptake is dictated by the maximum uptake rate, V_P^{max}, the half-saturation concentration k_P, and the ambient phosphate concentration P. The grazing rate, G_C, is a function of the available prey carbon biomass, F_C, and the half-saturation concentration for grazing k_g. Here, λ is the maximum prey assimilation efficiency, and the P:C ratio of prey items is denoted as Q_F.

Shift Toward Larger Cells. Assuming equilibrium, we can solve Eqs. 2 and 3 for $P = R_P^*$, which represents the minimum resource concentration required for the population to overcome the basal mortality m. For a phytoplankton population, R_P^* is simply a function of the organisms physiology, the light-limited growth rate V_C, and the mortality rate. Typically, in size-structured phytoplankton communities, R_P^* increases with organism size, such that the smallest phytoplankton are able to exclude larger groups that are outcompeted for scarce nutrients. For a mixotroph population, R_P^* is given by a very similar function, but we must also account for the ingestion of prey, as represented by $G_C = G_C^{max}[F_c/(F_c + k_g)]$:

$$R_P^* = \frac{k_P}{V_P^{max} \left(m Q_{min} \Delta Q \left[Q_{max} \left(1 - \frac{m}{V_C + G_C} \right) - Q_{min} \right]^{-1} - G_C \lambda Q_F \right)^{-1} - 1}. \tag{4}$$

On the right-hand side of Eq. 4, the terms $G_C \lambda$ and $G_C \lambda Q_F$ are unique to the mixotroph, whereas the other terms are common to the phytoplankton and mixotroph. Positive values for $G_C \lambda$ and $G_C \lambda Q_F$ will always decrease R_P^*, demonstrating that the additional carbon and phosphorus acquired by grazing both serve to make the mixotrophs more competitive.

Smaller Equilibrium P:C Quota. Eq. 2 can be solved to find the equilibrium P:C ratio, $\bar{Q}$:

$$\bar{Q} = \frac{Q_{min}}{1 - \frac{m}{(G_C \lambda + V_C)}}. \tag{5}$$

Eq. 5 gives the equilibrium stoichiometry of the cell when photosynthetic and predatory carbon assimilation are balanced by mortality. Relative to a specialist zooplankton (frequently dominant in the two-guild model), the additional carbon acquisition term V_C serves to decrease $\bar{Q}$ (i.e., increase C:P).

1. Hollowed AB, et al. (2013) Projected impacts of climate change on marine fish and fisheries. *ICES J Mar Sci* 70(5):1023–1037.
2. Hain MP, Sigman DM, Haug GH (2014) *The Biological Pump in the Past. Treatise on Geochemistry* (Elsevier, Oxford), 2nd Ed, pp 485–517.
3. Stoecker DK (1998) Conceptual models of mixotrophy in planktonic protists and some ecological and evolutionary implications. *Eur J Protistol* 34(3):281–290.
4. Stoecker DK (2009) Acquired phototrophy in aquatic protists. *Aquat Microb Ecol* 57(3):279–310.
5. Zubkov MV, Tarran GA (2008) High bacterivory by the smallest phytoplankton in the North Atlantic Ocean. *Nature* 455(7210):224–226.
6. Hartmann M, et al. (2012) Mixotrophic basis of Atlantic oligotrophic ecosystems. *Proc Natl Acad Sci USA* 109(15):5756–5760.
7. Flynn KJ, et al. (2013) Misuse of the phytoplankton-zooplankton dichotomy: the need to assign organisms as mixotrophs within plankton functional types. *J Plankton Res* 35(1):3–11.
8. Dugdale RC, Goering JJ (1967) Uptake of new and regenerated forms of nitrogen in primary productivity. *Limnol Oceanogr* 12(2):196–206.
9. Ward BA, Dutkiewicz S, Jahn O, Follows MJ (2012) A size structured food-web model for the global ocean. *Limnol Oceanogr* 57(6):1877–1891.
10. Fasham MJR, Sarmiento JL, Slater RD, Ducklow H, Williams R (1993) Ecosystem behavior at Bermuda Station "S" and OWS "India": A GCM model and observational analysis. *Global Biogeochem Cycles* 7(2):379–416.
11. Le Quéré C, et al. (2005) Ecosystem dynamics based on plankton functional types for global ocean biogeochemistry models. *Glob Change Biol* 11(11):2016–2040.
12. Stock CA, Dunne JP, John JG (2014) Global-scale carbon and energy flows through the marine planktonic food web: An analysis with a coupled physical–biological model. *Prog Oceanogr* 120:1–28.
13. Armstrong RA (1999) Stable model structures for representing biogeochemical diversity and size spectra in plankton communities. *J Plankton Res* 21(3):445–464.
14. Zubkov MV (2009) Photoheterotrophy in marine prokaryotes. *J Plankton Res* 31(9):933–938.
15. Johnson MD, Stoecker DK (2005) Role of feeding in growth and photophysiology of *Myrionecta rubra*. *Aquat Microb Ecol* 39(3):303–312.
16. Thingstad TF (1998) A theoretical approach to structuring mechanisms in the pelagic food web. *Hydrobiologia* 363(1):59–72.
17. Uitz J, Claustre H, Morel A, Hooker SB (2006) Vertical distribution of phytoplankton communities in open ocean: An assessment based on surface chlorophyll. *J Geophys Res* 111(C8):C08005.
18. Uitz J, Claustre H, Gentili B, Stramski D (2010) Phytoplankton class specific primary production in the world's oceans: Seasonal and interannual variability from satellite observations. *Global Biogeochem Cycles* 24(3):GB3016.
19. Edwards KF, Thomas MK, Klausmeier CA, Litchman E (2012) Allometric scaling and taxonomic variation in nutrient utilization traits and maximum growth rate of phytoplankton. *Limnol Oceanogr* 57(2):554–566.
20. Thingstad TF, Havskum H, Garde K, Riemann B (1996) On the strategy of "eating your competitor": A mathematical analysis of algal mixotrophy. *Ecology* 77(7):2108–2118.
21. Maranger R, Bird DF, Price NM (1998) Iron acquisition by photosynthetic marine phytoplankton from bacteria. *Nature* 396:248–251.
22. Smalley GW, Coats DW, Stoecker DK (2003) Feeding in the mixotrophic dinoflagellate Ceratium furca is influenced by intracellular nutrient concentrations. *Mar Ecol Prog Ser* 262:137–151.
23. Martiny AC, Vrugt JA, Lomas MW (2014) Concentrations and ratios of particulate organic carbon, nitrogen, and phosphorus in the global ocean. *Sci Data* 1:140048.
24. Teng Y-C, Primeau FW, Moore JK, Lomas MW, Martiny AC (2014) Global-scale variations of the ratios of carbon to phosphorus in exported marine organic matter. *Nat Geosci* 7(12):895–898.
25. Mitra A, et al. (2014) The role of mixotrophic protists in the biological carbon pump. *Biogeosciences* 11(4):995–1005.
26. Raven JA (1997) Phagotrophy in phototrophs. *Limnol Oceanogr* 42(1):198–205.
27. Våge S, Castellani M, Giske J, Thingstad TF (2013) Successful strategies in size structured mixotrophic food webs. *Aquat Ecol* 47(3):329–347.
28. Adams SM, Kimmel BL, Ploskey GR (1983) Sources of organic matter for reservoir fish production: A trophic dynamic analysis. *Can J Fish Aquat Sci* 40(9):1480–1495.
29. Winemiller KO (1990) Spatial and temporal variation in tropical fish trophic networks. *Ecol Monogr* 60(3):331–367.
30. Moore CM, et al. (2013) Processes and patterns of oceanic nutrient limitation. *Nat Geosci*, 10.1038/NGEO1765.
31. Redfield AC (1934) On the proportions of organic derivatives in sea water and their relation to the composition of plankton. *James Johnstone Memorial Volume*, ed Daniel RJ (Liverpool University Press, Liverpool, UK), pp 176–192.
32. Ward BA, Dutkiewicz S, Barton AD, Follows MJ (2011) Biophysical aspects of resource acquisition and competition in algal mixotrophs. *Am Nat* 178(1):98–112.
33. Ward BA, Dutkiewicz S, Follows MJ (2014) Modelling spatial and temporal patterns in size-structured marine plankton communities: Top-down and bottom-up controls. *J Plankton Res* 36(1):31–47.
34. Vallina SM, Ward BA, Dutkiewicz S, Follows MJ (2014) Maximal foraging with active prey-switching: A new "kill the winner" functional response and its effect on global species richness and biogeography. *Prog Oceanogr* 120(1):93–109.
35. Marañón E, et al. (2013) Unimodal size scaling of phytoplankton growth and the size dependence of nutrient uptake and use. *Ecol Lett* 16(3):371–379.
36. Droop MR (1968) Vitamin B12 and marine ecology, IV. The kinetics of uptake, growth and inhibition in *Monochrysis lutheri*. *J Mar Biol Assoc U K* 48(3):689–733.
37. Caperon J (1968) Growth response of *Isochrysis galbana* to nitrate variation at limiting concentrations. *Ecology* 49(5):866–872.
38. Flynn KJ (2008) The importance of the form of the quota curve and control of non-limiting nutrient transport in phytoplankton models. *J Plankton Res* 30(4):423–438.
39. Wroblewski JS (1977) A model of phytoplankton plume formation during variable Oregon upwelling. *J Mar Res* 35(2):357–394.
40. Dutkiewicz S, Follows M, Bragg JG (2009) Modeling the coupling of ocean ecology and biogeochemistry. *Global Biogeochem Cycles* 23(4):GB4017.
41. Geider RJ, MacIntyre HL, Kana TM (1998) A dynamic regulatory model of phytoacclimation to light, nutrients and temperature. *Limnol Oceanogr* 43(4):679–694.
42. Moore JK, Doney SC, Kleypas JA, Glover DM, Fung IY (2002) An intermediate complexity marine ecosystem model for the global domain. *Deep Sea Res Part II Top Stud Oceanogr* 49(1-3):403–462.
43. Bec B, Collos Y, Vaquer A, Mouillot D, Souchu P (2008) Growth rate peaks at intermediate cell size in marine photosynthetic picoeukaryotes. *Limnol Oceanogr* 53(2):863–867.
44. Wirtz KW (2011) Non-uniform scaling in phytoplankton growth rate due to intracellular light and CO_2 decline. *J Plankton Res* 33(9):1325–1341.
45. Dutkiewicz S, Ward BA, Monteiro FM, Follows MJ (2012) Interconnection of nitrogen fixers and iron in the Pacific Ocean: Theory and numerical simulations. *Global Biogeochem Cycles* 26(1):GB1012.
46. Marshall JC, Hill C, Perelman L, Adcroft A (1997) Hydrostatic, quasi-hydrostatic and non-hydrostatic ocean modeling. *J Geophys Res* 102(C3):5733–5752.
47. Wunsch C, Heimbach P (2007) Practical global ocean state estimation. *Physica D* 230(1-2):197–208.
48. Behrenfeld MJ, Falkowski PG (1997) Photosynthetic rates derived from satellite-based chlorophyll concentration. *Limnol Oceanogr* 42(1):1–20.
49. Conkright ME, et al. (2002) *World Ocean Atlas 2001* (NOAA Atlas NESDIS52, Washington, DC).
50. Tagliabue A, et al. (2012) A global compilation of dissolved iron measurements: Focus on distributions and processes in the Southern Ocean. *Biogeosciences* 9(6):2333–2349.
51. Kleypas JA, Doney SC (2001) *JGOFS Biogeochemical Properties in the Ocean Mixed Layer* (Research Data Archive at the National Center for Atmospheric Research, Computational and Information Systems Laboratory). Available at rda.ucar.edu/datasets/ds259.0/. Accessed July 16, 2010.